Case Study: Assessing Construction-Induced Deformations in Tailings Storage Facility Embankments

Mrunmay Junagade, Knight Piésold Consulting, Denver, Colorado, USA
 Jess Walker, Knight Piésold Consulting, Denver, Colorado, USA
 Sudhir Tripathi, Knight Piésold Consulting, Denver, Colorado, USA
 Jordan Scheremeta, Knight Piésold Consulting, Denver, Colorado, USA
 Jeffrey Coffin, Knight Piésold Consulting, Denver, Colorado, USA
 Paul Ridlen, Knight Piésold Consulting, Denver, Colorado, USA

Abstract

Tailings Management Facility (TMF) dams on mine sites are typically stage raised throughout the course of mining. This process begins with the construction of a starter dam, followed by later-stage raising using either downstream, centreline, or upstream construction, or a combination of these methods. Throughout the course of construction, deformations are expected to occur in the existing embankment due to the development of deviatoric and shear stresses from construction loading, which are a function of the shear and bulk modulus of the embankment fills. Mines often monitor these deformations with inclinometers and surface monuments installed on and through the crest and downstream embankment fills. The reasonableness of the resulting deformations is often evaluated based on experience and engineering judgment. In this study, a method is discussed for evaluating the reasonableness of inclinometer deformations during TMF raise construction, using a finite-difference numerical modelling approach. Stiffness parameters used in the numerical models are initially established using a laboratory-based approach, and these parameters are then compared with calibrated parameters based on historical deformation data at each of two TMF case studies. The calibrated models can then be used to assess the reasonableness of the existing deformations within TMF embankments and to predict expected deformations during future stage-raising.

Introduction

Mining sites generally adopt a staged methodology for constructing tailings dams. This approach typically involves constructing a starter dam followed by successive raises, using either upstream, downstream, centreline, or a combination of stage-raising methods. Staged construction allows for real-time performance

monitoring through instrumentation (e.g., piezometers, inclinometers, survey monuments, etc.), thereby facilitating design adjustments and modifications based on observed in-situ behaviour. This approach can be traced back to Terzaghi and Peck (1948), who designated it the "observational method."

Embankment instrumentation plays a key role in staged construction by providing data to evaluate embankment behaviour during construction and subsequent deposition. A well-designed instrumentation system tied to the observational method enhances safety and regulatory compliance throughout the dam's operational life. Instrumentation systems typically help establish deformation and pore pressure thresholds, which can be used to develop Trigger Action Response Plans (TARPs). The efficiency of the observational method depends on two components: (1) quality control of the data collected by the instrumentation system and (2) utilization of the collected data towards meaningful interpretations of embankment behaviour.

The two TMF dams covered in this study are outfitted with various types of instrumentation used in monitoring deformations (e.g., survey monuments, robotic total station monitoring prisms, inclinometers). Due to the stage-raising process used to construct both facilities, collecting a continuous embankment deformation dataset can be challenging. Surficial displacement monitoring equipment must be removed and reinstalled during each raise, resulting in discontinuous data that spans the operational lifespan of an individual raise. However, inclinometers are installed internally within the dams and can remain in place during the construction of subsequent stage raises, providing a more continuous picture of embankment deformation over time. As such, this case study focuses on high-quality in-situ deformation monitoring data from inclinometers installed in the two embankments for comparison with and calibration of the numerical models.

Inclinometers are the most common tool used at TMF dams for monitoring internal deformations. With proper quality control, the data can be reliable for monitoring embankment performance. At TMF dams, inclinometers typically consist of a hollow casing comprised of acrylonitrile butadiene styrene (ABS) plastic, pultruded fibreglass, or, in some instances, aluminum material, which is installed through the embankment fill and anchored in the underlying foundation bedrock (below the zone of influence of induced deformations). Surveys of the inclinometer casing are collected using an inclinometer probe equipped with accelerometers, which are pulled through the casing by a cable reel. In taking a survey, the probe is pulled through two sets of casing grooves, typically aligned perpendicular (A-direction) and parallel (B-direction) to the dam crest. Incremental readings are collected at a set interval (typically 0.5 metres) from the bottom to the top of the casing. The inclinometer probe collects incremental measurements of tilt angles, which are converted to incremental lateral deviations and then summed incrementally from the bottom to the top of the casing to obtain cumulative deviations. Cumulative deviations can then be plotted with depth to illustrate a casing profile (DGSI, 2011).

Deformation is assessed by obtaining cumulative deviation profiles with respect to a baseline survey that serves as a reference zero. This plot is commonly referred to as a profile change. Variations in the profile change from a baseline survey can be interpreted as lateral displacement of the inclinometer casing driven by deformation of the surrounding embankment fill; however, this inference is not always true. Inclinometer probes are sensitive and inherently prone to random and systematic data collection errors, including random errors; systematic error forms such as bias, sensitivity drift, rotation, and depth positioning errors; or one-off errors like misalignment of the probe within the casing grooves (Mikkelson, 2003). Anomalous surveys affected by these errors can easily be mistaken as signs of real embankment deformation, which can then cause artificial exceedances of set thresholds and lead to misleading interpretations of dam performance. Thus, it takes skilled field personnel, combined with robust screening and error correction during the data reduction process, to amass a high-quality inclinometer database reflective of actual embankment deformations. Common pitfalls in data quality, as well as established methods for data screening and error correction for the embankments covered in this case study, are discussed later in this paper.

Once reliable in-situ deformation data have been established, engineers can use Finite Element Method (FEM) or Finite Different Method (FDM) programs to perform inverse numerical analyses and evaluate the constitutive relationships of the embankment materials. Several advancements have been made in numerical modelling over the years to predict embankment deformations. One of the earliest models to capture the nonlinear stress-strain response and stress-dependent stiffness of soils was an elasticity-theory-based model, deemed the Hyperbolic-Soil model, and developed by Duncan and Chang (1970). Kovacevic (1994) showed that elastic-plastic constitutive models are well-suited to model rockfill embankment deformations. Subsequently, Shanz et al. (1999) presented the Hardening-Soil model, an extension of the Hyperbolic-Soil model, with a numerical elastoplastic framework that captured both shear and volumetric hardening behaviour of the soil.

The embankment deformations recorded in the installed instrumentation can be used to perform inverse analyses to optimize constitutive model parameters, enabling engineers to use the calibrated constitutive models to estimate deformation across multiple sections or stage raises for the embankments. Multiple researchers have demonstrated that inverse calibration of constitutive models—such as the Mohr-Coulomb, Hyperbolic, and Hardening Soil models—using in-situ instrumentation data is an effective method for predicting embankment behaviour (Bourdeau, 2004; Szostak-Chrzanowski & Massiéra, 2004; Aflaki, 2009; Pramthawee et al., 2011; Moussai, 2013; Rashidi & Haeri, 2017; Lashin et al., 2021; Farajniya et al., 2024). Other studies (e.g., Vahdati et al., 2014 and Toromanović et al., 2020) have used computationally intensive methods, such as genetic algorithms, to optimize the parametric analysis procedure to back-calculate the constitutive model parameters. Knuttson et al. (2018) showed the efficacy

of the Plastic-Hardening model in inverse analyses for tailing dams. This study used the Plastic-Hardening (Cheng et al., 2016) model—an extension of the Hardening-Soil model—to perform inverse analyses on two zoned earth-fill dams with Fast Lagrangian Analysis of Continua (FLAC) (Itasca, 2019). The rationale for selecting the constitutive model and the methodology used to calibrate its parameters with in-situ deformation data, as well as to extrapolate the calibrated model for predictive modelling, is described in subsequent sections of this paper.

In the aftermath of several high-profile tailings dam failures, regulatory scrutiny and public sensitivity around tailings dams have intensified globally. Calibrated and transparently reported dam performance data are essential to strengthening regulatory compliance and building credibility and trust among local communities, investors, and governing bodies. This case study is an outcome of efforts undertaken to answer an independent reviewer's question: "Can in-situ deformation data verify that the embankment is behaving as expected, and can it be used to predict future performance?" The objective of this paper is to describe the methodology adopted by the authors to use available in-situ deformation data from inclinometers installed within two tailings dams to assess the embankment performance through backanalysis using numerical modelling.

Project Background of the Two TMF Dams

This case study deals with two zoned earth-fill tailings dams primarily composed of two kinds of construction material. For confidentiality reasons and in accordance with client agreements, the names, specific locations, and detailed material zonation within the embankment of these two dams have been withheld. The dams are referred to as "Dam 1" and "Dam 2" throughout the paper to maintain project anonymity while still conveying lessons learned and engineering insights gained from the analyses performed.

Dam 1 is a cross-valley impoundment with the starter dam initially raised using the downstream method, followed by subsequent centreline construction raises. The embankment is primarily constructed using compacted local silty and clayey material. A representative particle size distribution curve is provided in Figure 1 for the material that forms the bulk of the embankment. While the presence of engineered zones such as drains, filters, and transitions is expected to affect the embankment's overall performance (e.g seepage, stability, etc.), the stress-strain deformation of the structure is anticipated to be primarily governed by the main embankment material (i.e., the compacted silt material). The height of the embankment above the foundation is currently 120 metres (m), and the maximum height at life of mine (LOM) is anticipated to be 125 m above the foundation. A typical cross-section for Dam 1 is shown in Figure 2.

Dam 2 is a zoned earth-fill embankment that spans two valleys and was also initially constructed as a downstream raised facility, followed by centreline raises. A fundamental difference is that the embankment

for Dam 2 is built using compacted waste rock and will be significantly taller than Dam 1 at LOM configuration. Dam 2 also consists of engineered zones, such as a filter and transition, that make up a small portion of the embankment. Figure 1 shows a representative particle size distribution plot of the compacted waste rock. Figure 3 shows a typical section of Dam 2. The current height of Dam 2 is approximately 160 m, and the maximum height at the end of mine life is projected to be 220 m.

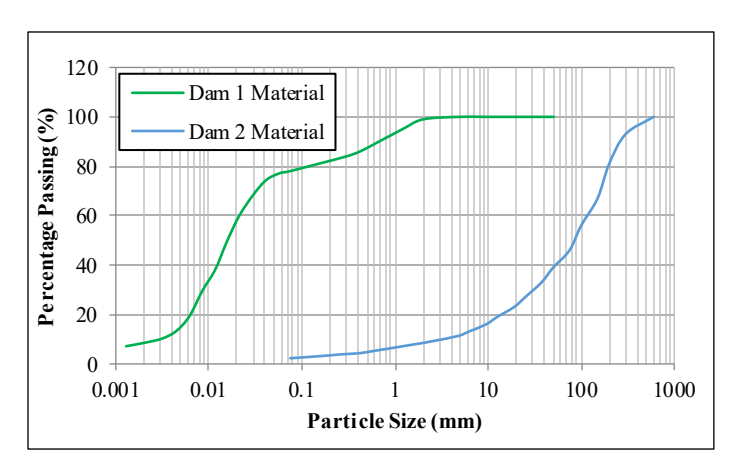


Figure 1: Representative PSD curve for the main embankment material of Dam 1 and Dam 2

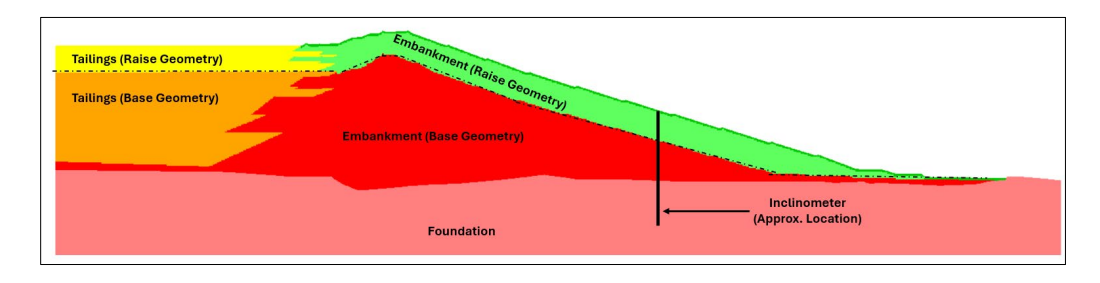


Figure 2: Typical cross-section of Dam 1

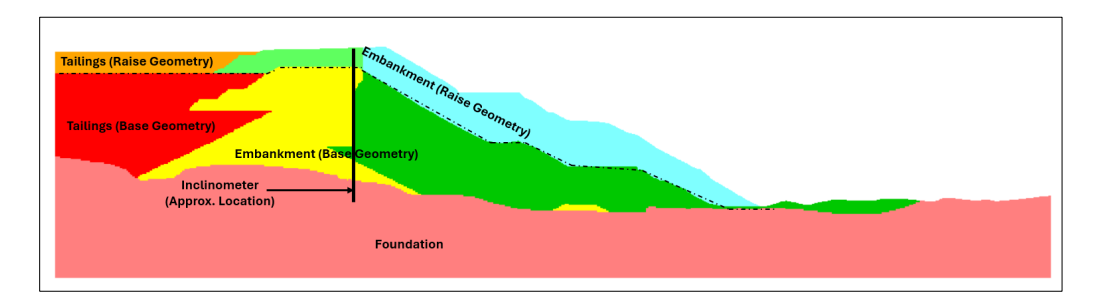


Figure 3: Typical cross-section of Dam 2

Inclinometer Data Analysis and Quality Control

Developing meaningful inclinometer data starts with proper data quality control, which requires robust data screening and data reduction techniques. For the two embankments covered herein, two-pass surveys are

initially used for data smoothing. Inclinometer readings are taken in two inverse probe orientations in each set of grooves for a total of four passes per inclinometer survey (A0, A180, B0, and B180); an algebraic difference (of the raw probe units) is then taken between the corresponding 0- and 180-orientation readings and divided by two prior to calculating profile change. When plotted, the sum between the 0- and 180-direction readings becomes a valuable tool for data quality screening, deemed a checksum plot. For these diagnostic plots, uniform vertical data is the desired outcome. Irregularities in the checksum can be attributed to casing groove conditions, probe performance, or operator error in data collection (or a combination of these factors). Consistent irregularities may indicate a combination of systematic and random errors in data collection or groove condition, whereas one-off irregularities can suggest problems with data collection, excess random errors, or newly formed systemerrors. Checksum plots for inclinometer readings from Dam 1 and Dam 2 are cross-referenced during data reduction and analysis. Any atypical profile change patterns are compared against the corresponding checksum plots.

A high-quality baseline reading is key to calculating reliable profile-change data. Checksums are used in establishing high-quality baselines for each inclinometer at Dams 1 and 2. Several baseline readings are collected following installation of an inclinometer casing (after allowing ample time for grout curing) or introduction of a new probe. The reading with the most uniform checksum, assumed to represent the highest quality survey, is selected as the baseline. It should be noted that it is best practice in data reduction to use the same probe that collected the baseline reading to collect subsequent data. Since different probes have different factory calibration constants, sensitivities, and sensor axis alignments, profile changes between a baseline survey and a survey collected with different probes can introduce significant errors (often rotational error) into the calculated value, resulting in incompatibility with previous profile-change data. Therefore, all inclinometer data from Dams 1 and 2 are analyzed against baseline surveys from the same probe. Whenever a probe breaks, each inclinometer is re-baselined using the replacement probe. Unfortunately, this approach results in a reset of the profile-change dataset, leading to a loss in continuity of the deformation data timeline. Inclinometers are also re-baselined after the development of any type of systematic error that is not easily and reliably corrected for, such as depth positioning error.

During analysis, each reading is evaluated for systematic errors, which tend to be readily identifiable through distinctive data patterns. Aside from a few one-off instances of depth positioning error at Dam 1 due to telescopic casing segment collapse (addressed via re-baselining to readings following the collapse), the only systematic error regularly identified in the data is bias shift error. Bias shift correction is applied as necessary to each reading during data reduction according to the methodology detailed in Mikkelsen (2003). Proper application of bias shift correction is critical, and it requires an experienced data analyst to ensure that corrections are not over-applied. Generally, for Dams 1 and 2, bias shift correction is applied to ensure that readings achieve a reasonable profile-change fit with historical data. The focus is on aligning

the portion of the inclinometers anchored in bedrock, where deformation is not expected, and maintaining consistency in the inclinometer data. It should be noted that the portion of the inclinometer readings corresponding to the foundation is a useful tool for data quality screening, as profile changes indicating deformation within the bedrock often signify a poor-quality survey.

Given that these TMF dams are stage raised, the inclinometer casings must be extended with each raise, which has been one of the main historical challenges with inclinometer monitoring at these sites. Placing the overlying embankment fill and the associated casing extension increases the axial loading of the inclinometer column, often leading to small buckling patterns developing in the profile changes at the location of casing segment joints. Furthermore, for five of the six inclinometers in this study, which are comprised of antiquated aluminum casings, loading from casing extension eventually triggered obstruction of the inclinometer casings at discrete points, resulting in full or partial losses of instrument functionality. One of these obstructions, as captured through a video inspection, is shown in Figure 4.

As such, it is vital to highlight the importance of using industry-standard casing materials (ABS plastic, which comprises the inclinometer at Dam 1 Section D in this study, and pultruded fibreglass), proper installation procedures, and general caution during inclinometer extension to minimize extension effects (minor buckling at joints) or worse. The backfill around casing extensions should also be compacted appropriately to reduce differential settlement between the backfill and the surrounding embankment fill. Augmentation of the downstreamstrain in the profile change is also often seen following casing extensions. However, this strain is primarily considered to be a result of embankment deformation from construction loading following the stage raise.

To attempt to prolong instrument life, axial loading development can potentially be mitigated using telescopic casing segments; however, as these casings collapse (which can be induced upon casing extensions), it introduces a depth positioning error into the dataset, which is difficult to correct for. The depth position error was a specific challenge encountered with the inclinometer at Dam 1 Section D. After the error developed and the associated telescopic segment collapsed, the instrument was re-baselined.

Typically, profile-change variances due to poor-quality survey data will exhibit unreasonable patterns and/or corresponding checksum variances; however, confirmatory re-readings are requested upon any instance of large profile-change variances or anomalous patterns, regardless of whether there is a checksum variance. If the re-reading no longer shows the anomalous pattern, the original reading is discarded, and its variances are attributed to poor-quality data. However, if the re-reading continues to show the variance, the original reading quality is validated, and the profile-change variation can be interpreted as real deformation of the inclinometer casing. This procedure of screening and requesting confirmatory re-readings has generally resulted in a high-quality profile-change dataset for each facility, providing a high level of

confidence that the profile-change data represent true internal deformation patterns and strain magnitudes within the embankments.



Figure 4: Aluminum inclinometer casing obstruction, Dam 1 Section A

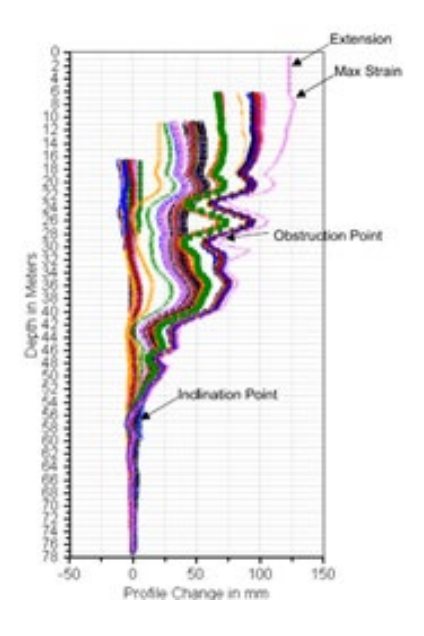


Figure 5: Historical profile change data, Dam 1 Section A

Case Study Inclinometer Data

Figure 5 presents the full set of high-quality historical A-direction (perpendicular to crest) profile-change data for the inclinometer installed in Section A at Dam 1. Figures 10 through 15 present the A-direction profile-change data for the final inclinometer readings evaluated from the six inclinometers along different sections at Dams 1 and 2, and the results of numerical modelling. B-direction data are not considered herein, since the 2-D plane-strain numerical models used in this study can only evaluate lateral embankment

deformations. Figure 5 highlights the key features of the inclinometer profile-change pattern shared by most of the inclinometers in this study.

In general, the six inclinometers present a gradual development of downstream deformation augmented with each stage raise due to loading from additional fill placement. This gradual development is clearly illustrated through the series of historical readings in Figure 5, with instances of extensions marking the stage-raise timeline. As expected, all inclinometers exhibit close alignment to the baseline readings through the foundation. A clear inclination point is observed approximately at the interface of the embankment fill materials and the foundation, due to the marked increase in stiffness at the foundation contact. Distinct buckling features in the profile-change patterns are apparent in the data near casing joints, the most prominent of which are seen at the inclinometers at Dam 1 Section A and Dam 2 Sections A and B. The larger magnitude buckling at the Dam 2 inclinometers is attributed to the embankment rockfill, which is assumed to generate greater stresses on the inclinometer casing joints than the compacted silt fill at Dam 1.

However, the extent of buckling may also reflect the level of care taken by the construction team during stage-raise casing extensions, the overall quality of the installation (casing assembly, grouting, etc.), and the difference in severity of weathering of the aluminum casing between the two facilities. Casing obstructions occurred for five of the six inclinometers in this study, with only the inclinometer at Dam 1 Section D, comprised of ABS plastic rather than aluminum, remaining unobstructed. Figure 5 calls out the obstruction point at a depth of 29.5 m, which ended the life of the Dam 1 Section A inclinometer. An image of this obstruction is shown above in Figure 4. Data for each inclinometer of this study are described below: The inclinometer data from Dam 1 Section A cover a timeline of three-stage raises (covering the addition of 13 m total of compacted silt fill to the embankment) and show a maximum A-direction downstream displacement from the baseline reading of 125 millimetres (mm).

- The inclinometer data from Dam 1 Sections B and C cover a timeline of four-stage raises (covering the addition of 16 m of compacted silt fill to the embankment). The inclinometer at Section B shows a maximum A-direction downstream displacement of 87 mm, and the inclinometer at Section C shows a maximum A-direction downstream deformation of 65 mm.
- The inclinometer data from Dam 1 Section D cover a single stage raise (covering the addition of 3 m total of compacted silt fill to the embankment) and show a maximum A-direction downstream displacement of 23 mm.
- The inclinometer data from Dam 2 Sections A and B cover a timeline of two-stage raises (covering the addition of 15 m of rockfill to the embankment). The inclinometer at Section A shows a maximum A-direction downstream displacement of 276 mm, and the inclinometer at Section C shows a maximum A-direction downstream displacement of 200 mm.

Constitutive Modelling

An appropriate constitutive model was selected based on the need to predict deformations within an existing embankment due to placement of stage raises and the need to calculate horizontal and vertical displacements while accounting for (1) non-linearity in stress-strain response of soil, (2) stiffness degradation with shearing, and (3) an increase in stiffness under increased mean effective stresses. The Plastic-Hardening model available in FLAC (Itasca, 2019) is formulated within the elasto-plastic constitutive framework, incorporating a non-associated flow rule and a stress-dependent yield surface.

The hardening response is governed by accumulated plastic shear and volumetric strains, which allow the yield surface to expand under progressive loading. A Mohr-Coulomb failure criterion defined by cohesion and friction angle value is used. Relevant parameters of the plastic hardening model are presented in Table 1.

The most critical aspects of this constitutive model for modelling stage raising are the stiffness parameters, secant modulus, and oedometer modulus, described in Equations (1) and (2). As the model iteratively marches towards equilibrium, the modulus values are updated during the accumulation of strains and evolution of stresses (σ_3 in the equations). A detailed mathematical framework is available in Cheng and Detournay (2016).

$$E_{50} = E_{50}^{\text{ref}} \left(\frac{c \cot(\Phi') - \sigma_3}{c \cot(\Phi') + p^{\text{ref}}}\right)^m \text{(Equation 1)} \qquad E_{\text{oed}} = E_{\text{oed}}^{\text{ref}} \left(\frac{c \cot(\Phi') - \sigma_3}{c \cot(\Phi') + p^{\text{ref}}}\right)^m \tag{Equation 2)}$$

The model parameters were initially estimated by calibrating the model to laboratory triaxial tests. Deformations recorded by the inclinometers are essentially a drained response of the embankment materials. If excess pore pressures are developed due to placed construction lifts, they dissipate over time. Therefore, calibrating the model using high-quality Isotropically Consolidated Drained (ICD) tests forms the basis for the modelling approach. The calibration aims to reproduce, to the greatest extent possible, the deviatoric and volumetric stress-axial strain behaviour; the methodology was adopted as described by Cheng and Lucarelli (2016). For the Silty Material from Dam 1, 4-point ICD testing on 3-inch samples was completed. Two sets of 3-point ICD Triaxial testing were performed for the Rockfill Material at Dam 2.

The first set was performed on 1-metre diameter samples, and the second set on 6-inch samples with a parallel gradation. The calibrated values for embankment materials of both dams are presented in Table 2, and a single-element simulation compared to laboratory testing results is presented in Figure 6 through Figure 8.

Table 1: Plastic Hardening Model Parameters

| Parameter | Description |
|---------------------------------|---|
| c | Cohesion criteria in the Mohr-Coulomb strength envelope |
| Ψ | Dilation Angle |
| m | Power exponent for stress-dependency equation for stiffness |
| Rf | Failure Ratio |
| OCR | Overconsolidation ratio |
| ν | Poisson's ratio |
| Φ ' | Friction angle in the Mohr-Coulomb strength envelope |
| p^{ref} | Reference pressure (1 atm = 101.325 kPa) |
| $E_{50}{}^{\rm ref}$ | Reference secant modulus at 50% of max. deviatoric stress at the reference pressure. It mainly controls the shear strain response |
| $E_{ur}{}^{ref} \\$ | Reference unloading/reloading modulus at the reference pressure |
| $E_{\text{oed}}{}^{\text{ref}}$ | Reference oedometer modulus at the reference pressure. It mainly controls volumetric strain response |

The calibrated parameters generally captured the strength envelope and deviator stress-axial strain relationship effectively. However, the volumetric strain-axial strain relationship was more difficult to capture, especially at strains greater than 5%. The friction angles remained constant across all testing datasets for Dam 1 material. In contrast, for Dam 2, the strength (friction angles) degraded with increasing confining stress, as expected for rockfill that undergoes particle crushing at higher stresses (Leps, 1970). Poisson's ratio was estimated from Knc, which was estimated as $1-\sin(\phi')$ after Jaky (1944). A relationship was developed between friction angles and confining stress from the calibrated models, which will be used in actual simulations on the geometry. E_{ur}^{ref} was estimated to be three times E_{50}^{ref} as recommended by Lucarelli and Cheng (2016).

Table 2: Constitutive Model Parameters Calibrated from ICD Triaxial Testing

| Material | Confining Stress Kpa | E ^{ref} Fa | E ^{ref} Pa | E ^{ref} Pa | m | Rf | Φ' Deg. | Ψ Deg. | Knc | v |
|------------------------|----------------------------|------------------------|------------------------|------------------------|------|------|----------------|-----------|----------------------|--|
| Dam 1 (3-inch ICD) | 100, 400, 800, 1,350 | 12e6 | 36e6 | 5e6 | 0.80 | 0.80 | 31 | 0 | 0.45 | 0.31 |
| Dam 2 (6-inch ICD) | 100 1,000 2,000 | 22e6 | 66e6 | 8e6 | 0.65 | 0.75 | 42 36 34 | 0 | 0.27 0.31 0.32 | 0.21 0.24 0.24 |
| Dam 2 (1-metre ICD) | 100 1,000 2,000 | 40e4 | 120e6 | 12e6 | 0.70 | 0.70 | 43 41 41 | 16 0 | 0.27 0.31 0.31 | 0.210.240.24 |

Modelling Methodology

After developing initial parameters, the model was solved for the critical section geometry using the initial set of parameters, and the model deformations were compared to in-situ deformation data. Each numerical model started with a geometry built from as-built drawings corresponding to the point in time when the earliest inclinometer data were available or when the inclinometer was baselined. The model was then solved for static deformations and the displacements, followed by resetting the displacements and velocities to zero, thereby saving the stress state without deformations. Subsequently, the stage geometry corresponding to the last available inclinometer data was generated over the base geometry and solved for static load deformations. The horizontal deformations at the inclinometer location were then extracted from the model and compared to in-situ data. If the deformations mismatched, the model parameters $E_{50}^{\rm ref}$ and $E_{oed}^{\, ref}$ for the embankment that controls the shearing and volumetric strain response in the model were modified by trial and error until the model deformations were in reasonable agreement with the in-situ data in terms of deformation trends and magnitudes. The tailings and foundation parameters remained constant since these parameters were not expected to have a significant influence on embankment behaviour. The other modelling parameters were kept constant since it is assumed that the above two parameters primarily govern the embankment behaviour. The horizontal and vertical deformations in the embankment are a function of both shearing of the material and volumetric contraction due to an increase in mean stresses. Figure 9 shows the modelling methodology adopted in this study. Once the parameters were recalibrated using in-situ deformation data for one section's geometry, they were used to model multiple sections or stage raises where inclinometer data were available.

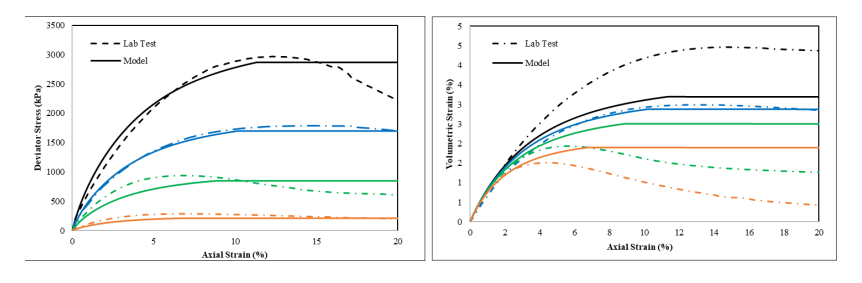


Figure 6: Single-element calibration for Dam 1 material

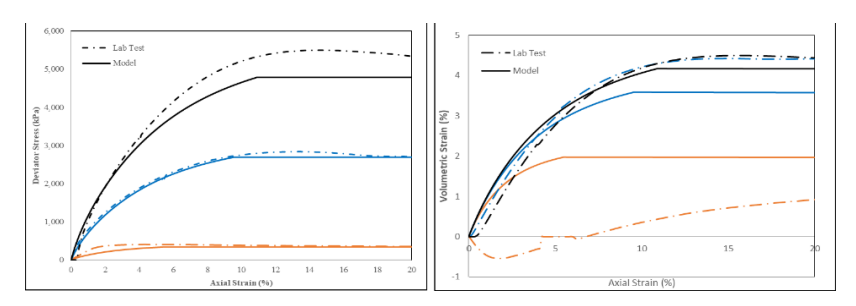


Figure 7: Single-element calibration for Dam 2 material (6-inch triaxial tests)

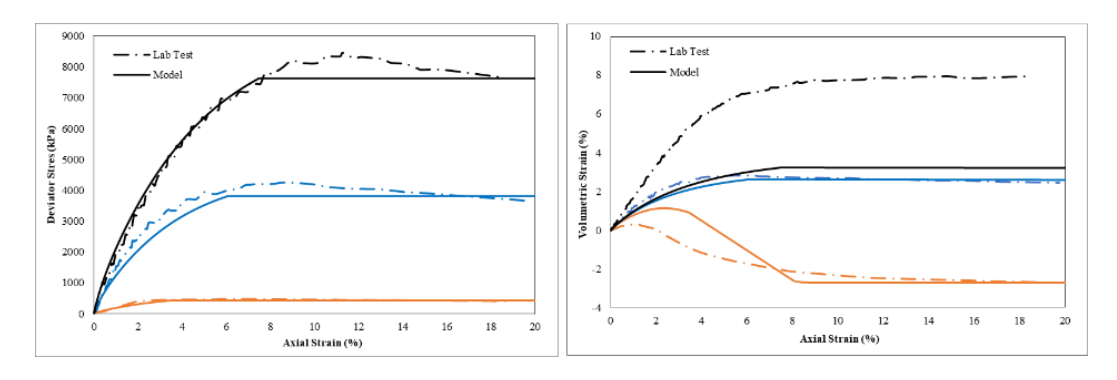


Figure 8: Single-element calibration for Dam 2 material (1-metre triaxial tests)



Figure 9: Modelling methodology

Results and Discussion

The parameters obtained from drained triaxial tests for Dam 1 were initially used to model the critical Section A. The height of the embankment for the base geometry was 97 m, and a centreline raise of 16 m was placed over the base geometry over four years. The initial E_{50}^{ref} and E_{oed}^{ref} parameters were stiffened by 60% to match the in-situ deformation data. These calibrated parameters were then used to model Sections B and C for Dam 1, with the base and final geometries corresponding to the same construction raises as Section A. The results are presented in Figures 10 through 12.

The same calibrated parameters were then used to model Section D, which represented construction stages for a one-year timeline, starting two years after the timeline used for Sections A, B, and C. The results for this model are presented in Figure 13. The calibrated model generally captures the trend well across all four sections, and the magnitude of deformations in the model is within +/- 50 mm of the in-situ deformations.

The Dam 2 embankment height for base geometry was 115 m, and the final geometry included a centreline raise of 15 m placed over the base geometry over two years. The calibrated parameters for Dam 2 were chosen as a composite between the properties obtained from 6-inch and 1-m triaxial tests. The stiffness properties from the 1 m drained triaxial test appeared to capture the embankment behaviour best; however, to incorporate conservatism (in terms of failure criteria), the strength envelopes derived from the 6-inch triaxial tests were used in the final calibrated model. Eref over the stightly reduced to obtain a better fit.

Since the model does not update friction angles as the stresses evolve, the friction angles were calculated based on estimated mean effective stresses from a clone model solved with simple constitutive relationships. After solving, the calibrated model was used to model another section for Dam 2 (Section B) with the same constructed raises, and the results are presented in Figures 14 and 15. The calibrated model parameters are presented in Table 3. For Dam 2, the numerical model deformations were within +/- 50 mm, excluding the top 20 m.

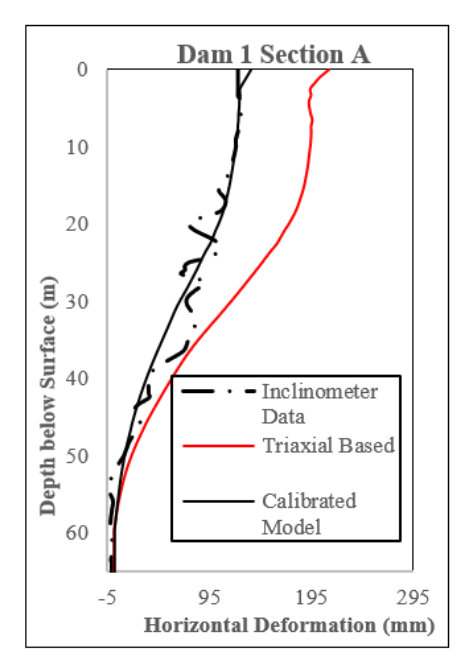


Figure 10: Dam 1 Section A results

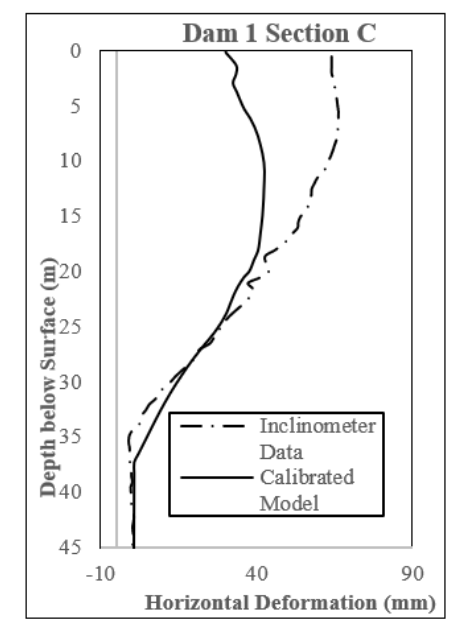


Figure 12: Dam 1 Section C results

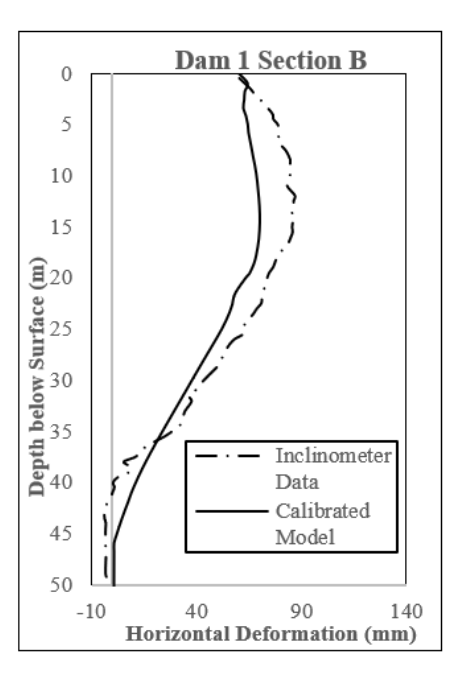


Figure 11: Dam 1 Section B results

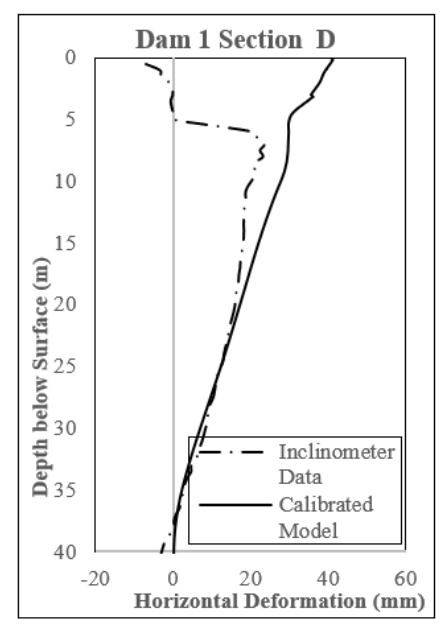
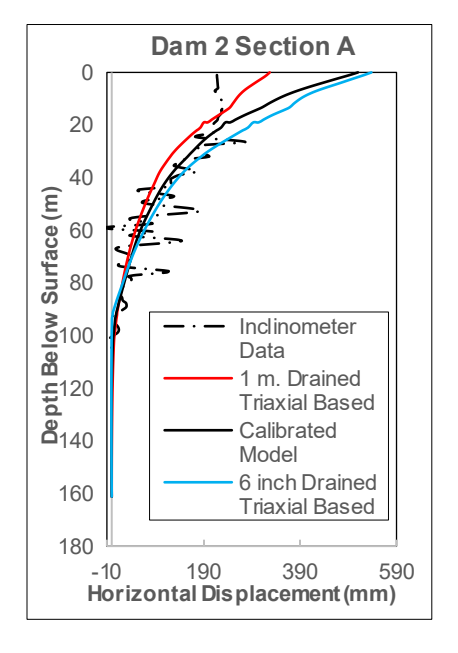


Figure 13: Dam 1 Section D results

Table 3: Parameters Calibrated from In-Situ Deformation Data

| Location | E ^{ref} Pa | E ^{ref} Pa | E ref oed Pa | m | Rf | Φ' Deg. | Ψ Deg. | Knc | v |
|----------|------------------------|------------------------|--------------------|------|------|----------------------------|-----------|------|------|
| Dam 1 | 19.2e6 | 57.6e6 | 8e6 | 0.80 | 0.80 | 31 | 0 | 0.45 | 0.31 |
| Dam 2 | 35e6 | 105e6 | 8e6 | 0.65 | 0.65 | (Varying with mean stress) | 0 | 0.25 | 0.34 |



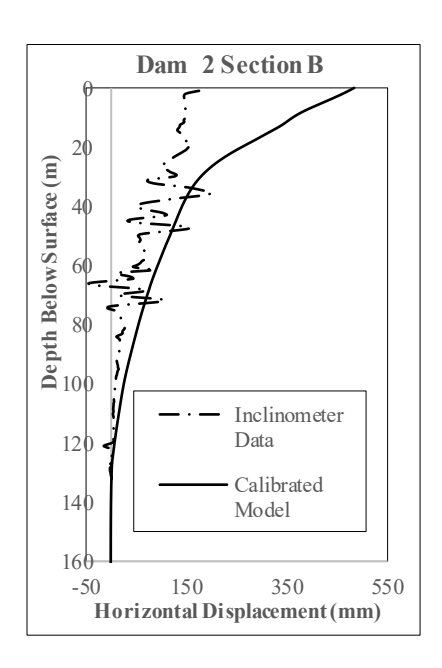


Figure 14: Dam 2 Section A results

Figure 15: Dam 2 Section B results

Available shear wave velocity data for the embankment materials for both dams were used to verify the reasonableness of the calibrated stiffness parameters. The reference small strain moduli ($E_0^{\rm ref}$) were calculated using the small strain shear modulus (G_0), which was calculated from shear wave velocity and density. Relevant calculations are shown in the appendix. The ratio of reference small strain moduli to calibrated reference secant moduli ($E_0^{\rm ref}/E_{50}^{\rm ref}$) was calculated to be 13.63 and 21.04 for Dams 1 and 2, respectively, while the ratio of reference secant moduli to calibrated reference tangent oedometer moduli ($E_{50}^{\rm ref}/E_{\rm oed}^{\rm ref}$) was calculated to be 2.4 and 4.38 for Dams 1 and 2, respectively. These values align well with the industry-standard practice of reducing the small-strain moduli by an order of magnitude to obtain large-strain moduli.

Conclusion

For TMF dams, inclinometers prove to be an effective tool for providing continuous internal deformation data, even as dams undergo successive stage raises, provided that the inclinometers are carefully extended. With high-quality installation, careful data collection, and proper quality screening and data reduction

techniques, inclinometers can facilitate an understanding of the embankment's mechanical behaviour, enabling real-time performance monitoring and decision-making. Despite challenges imposed by stage raising and outdated casing materials, the inclinometers highlighted in this case study clearly demonstrate their value in assessing construction-induced deformations through multiple stage raises.

Stage raising is a unique challenge in inclinometer monitoring at TMFs. Its negative impacts on the resulting data are not entirely avoidable; however, they can be reduced through proper installation, careful extension procedures, and the use of suitable casing materials. Aluminum inclinometer casing is common at older TMF facilities, and five of the six inclinometers in this study were comprised of this material. Based on the inclinometers highlighted in this study and general experience with aluminum inclinometer casing, installations of this type are likely to become obstructed after multiple cycles of seasonal weathering. This results in weakened casing points, deformations from the stage raising of a dam, and axial loading from casing extensions behaving as an obstruction-triggering mechanism. As such, aluminum casing is not optimal for long-term monitoring of inclinometer installations at large TMF dams. Based on the performance of the inclinometer at Dam 1 Section D, as well as several other inclinometers at this location, installations consisting of current industry-standard ABS-plastic and pultruded-fibreglass components are better suited for long-term deformation monitoring at stage-raised TMFs. Furthermore, telescopic sections may be useful in prolonging the life of inclinometers and potentially alleviating some of the axial loading from casing extensions. However, as these segments collapse, they introduce a depth positioning error into the dataset, which is not easily correctable.

The numerical modelling calibration for the Plastic-Hardening constitutive model parameters reasonably captured both the magnitude and pattern of deformation in sections across both dams, using different types of embankment materials. While model results varied considerably for the top few metres of the embankment, the authors believe that the inclinometer data in this area are unreliable. This mismatch can be attributed to the uncertainty due to manual compaction in the vicinity of the inclinometer casing and insufficient care during casing extension. Given that the embankment materials were placed compacted, variation in modulus values due to apparent overconsolidation can also contribute to the mismatch of model deformations near the ground surface.

While modelling accuracy can be improved by calibrating with both horizontal displacement data from inclinometers and vertical displacement data from an array of settlement plates, obtaining continuous and reliable in-situ settlement data is often a challenge. In the absence of laboratory testing data, small-strain shear moduli calculated from in-situ measurements, such as shear wave velocity (Vs), can be used to estimate the stiffness parameters of the constitutive model. However, estimating the magnitude of reduction of small-strain shear modulus suitable for strain levels encountered in the field remains a challenging task.

This study shows that the reduction of small-strain moduli by an order of magnitude is a reasonable approach for the initial approximation of stiffness parameters (refer to the appendix for additional details).

Acknowledgements

The authors would like to express their sincere gratitude to Knight Piésold, Denver, for their support and to all colleagues involved for their invaluable guidance and contributions to this project.

References

- Aflaki, E. (2009). Comparing numerical analysis predictions and experimental data for Shirindarreh embankment earth dam. *Asian Journal of Applied Sciences*, 2(1), 50–62.
- Bourdeau, P. L. (2004). Long-term deformation of soft ground at a trial embankment site and its simplified numerical modeling. In *Geotechnical engineering for transportation projects* (pp. 968–975). American Society of Civil Engineers.
- Cheng, Z., & Detournay, C. (2016). Plastic hardening model I: Implementation in FLAC3D. In *Applied numerical modeling in geomechanicJunagades—2016* (Paper 04-02). Itasca International Inc.
- Cheng, Z., & Lucarelli, A. (2016). Plastic hardening model II: Calibration and validation. In *Applied numerical modeling in geomechanics*—2016 (Paper 06-03, pp. 393–396). Itasca International Inc.
- Duncan, J. M., & Chang, C. Y. (1970). Nonlinear analysis of stress and strain in soils. *Journal of the Soil Mechanics and Foundations Division*, 96(5), 1629–1653.
- Durham Geo Slope Indicator [DGSI]. (2011). Digitilt inclinometer probe manual.
- Farajniya, R., Poursorkhabi, R. V., Zarean, A., & Dabiri, R. (2024). Analysis and monitoring of the behavior of a rock fill dam ten years after construction: A case study of the Iran-Madanidam. *Geoenvironmental Disasters*, 11, 30. https://doi.org/10.1186/s40677-024-00295-4
- Itasca Consulting Group, Inc. (2019). FLAC—Fast Lagrangian analysis of continua (Version 8.1). Itasca Consulting Group, Inc.
- Jaky, J. (1944). The coefficient of earth pressure at rest. *Journal of the Society of Hungarian Architects and Engineers*, 78, 355–358.
- Knutsson, R., Viklander, P., & Knutsson, S. (2018). Benefits of advanced constitutive modeling when estimating deformations in a tailings dam. *Journal of Earth Sciences and Geotechnical Engineering*, 8(1), 1–19.
- Kovacevic, N. (1994). Numerical analysis of rockfill dams, cut slopes and road embankments [PhD thesis]. Imperial College, University of London.

TAILINGS AND MINE WASTE 2025 • BANFF, CANADA

- Lashin, I., Verret, D., Ghali, M., & Karray, M. (2021). Investigation of small- to large-strain moduli correlations of rockfill materials—Application to Romaine-2 Dam. *Canadian Geotechnical Journal*, 58(8), 1213–1230.
- Leps, T. M. (1970). Review of shearing strength of rockfill. *Journal of the Soil Mechanics and Foundations Division*, 96(SM4), 1159–1170.
- Lucarelli, A., & Cheng, Z. (2016). Plastic hardening model III: Design application. In *Applied numerical modeling* in geomechanics—2016 (Paper 06-04). Itasca International Inc.
- Mikkelsen, P. E. (2003). Advances in inclinometer data analysis. In Symposium on Field Measurements in Geomechanics (FMGM), Oslo, Norway, September 23–26.
- Moussai, B. (2013). Numerical analysis of El Agrem concrete face rockfill dam. Soils & Rocks, 36(3), 293-298.
- Pramthawee, P., Jongpradist, P., & Kongkitkul, W. (2011). Evaluation of hardening soil model on numerical simulation of behaviors of high rockfill dams. *Songklanakarin Journal of Science and Technology*, 33(3), 325–334.
- Rashidi, M., & Haeri, S. M. (2017). Evaluation of behaviors of earth and rockfill dams during construction and initial impounding using instrumentation data and numerical modeling. *Journal of Rock Mechanics and Geotechnical Engineering*, 9(4), 709–725.
- Schanz, T., Vermeer, P., & Bonier, P. (1999). Formulation and verification of the Hardening Soil model. In *Beyond* 2000 in computational geotechnics. Balkema.
- Szostak-Chrzanowski, A., & Massiéra, M. (2004). Modelling of deformations during construction of a large earth dam in the La Grande Complex, Canada. *Technical Sciences*, 7, 109–117.
- Terzaghi, K., & Peck, R. B. (1948). Soil mechanics in engineering practice. John Wiley & Sons.
- Toromanović, J., Mattsson, H., Knutsson, S., & Laue, J. (2020). Parameter identification for an embankment dam using noisy field data. In *Proceedings of the Institution of Civil Engineers—Geotechnical Engineering*, 173(6), 519–534.
- Vahdati, P., Levasseur, S., Mattsson, H., & Knutsson, S. (2014). Inverse hardening soil parameter identification of an earth and rockfill dam using genetic algorithm optimization. *Electronic Journal of Geotechnical Engineering*, 19, 3327–3349.

Appendix

Using the theory of elasticity, we can get E_0 as shown in Equation 3. Lucarelli and Cheng (2016) proposed the stiffness parameter estimations shown in Equations 4 and 5:

$$E_0 = 2(1 + v)G_0$$
 (Equation 3), $E_{ur} = E_0/(2 \text{ to 5})$ (Equation 4), $E_{50} = E_{ur}/(2 \text{ to 5})$ (Equation 5)

The tangent oedometer stiffness modulus E_{oed} is often assigned the same value as E_{50} , which might not necessarily be correct, as seen in the modelling exercise in this study. Shear Wave Velocity testing performed on the embankment materials for Dams 1 and 2 is shown in Figure A1.

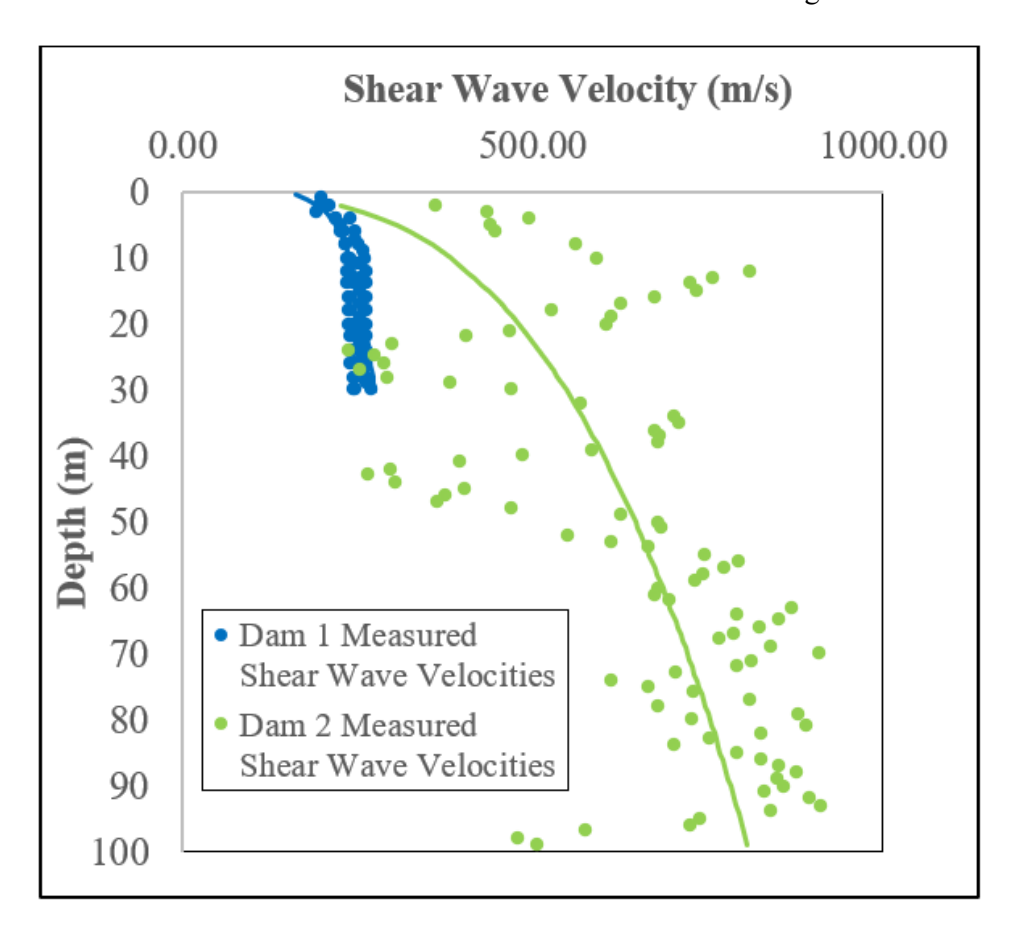


Figure A1: Shear wave velocities measured at Dam 1 and Dam

The measured shear wave velocities were used to find the small-strain shear modulus, and a best fit was developed using a power function similar to equations (2) and (3), as shown in Equation (6)

$$G_0 = G_0^{\text{ref}} (\frac{\sigma_3}{p^{\text{ref}}})^m$$
 – (assuming no cohesion) (Equation 6)